Functionally impaired RPL8 variants associated with Diamond–Blackfan anemia and a Diamond–Blackfan anemia-like phenotype

Simon Lebaron, Marie-Françoise O'Donohue, Scott Smith, Kendra Engleman, Jane Juusola, Nicole Safina, Isabelle Thiffault, Carol Saunders, Pierre-emmanuel Gleizes

Isabelle Thiffault ORCID iD: 0000-0001-7987-6731
Pierre-Emmanuel Gleizes ORCID iD: 0000-0003-0830-7341

Functionally impaired *RPL8* variants associated with Diamond-Blackfan anemia and a Diamond-Blackfan anemia-like phenotype

Simon Lebaron[1¶], Marie-Françoise O'Donohue[1¶], Scott C. Smith[2¶¤a], Kendra L. Engleman[3,4], Jane Juusola[6], Nicole N. Safina[3,4 ¤b], Isabelle Thiffault[2,5,7], Carol J. Saunders[2,5,7&*], Pierre-Emmanuel Gleizes[1&*]

[1] Molecular, Cellular and Developmental biology department (MCD), Centre de Biologie Intégrative (CBI), University of Toulouse, CNRS, UT3, Toulouse, France

[2] Department of Pathology and Laboratory Medicine, Children's Mercy Hospital, Kansas City, MO, USA

[3] Division of Clinical Genetics, Children's Mercy Hospital, Kansas City, MO, USA

[4] Department of Pediatrics, Children's Mercy Hospital, Kansas City, MO, USA

[5] University of Missouri-Kansas City School of Medicine, Kansas City, MO, USA

[6] GeneDx Inc, Gaithersburg, MD, USA

[7] Center for Pediatric Genomic Medicine, Children's Mercy Hospital, Kansas City, MO, USA

* **Corresponding authors**: Pierre-Emmanuel Gleizes, pierre-emmanuel.gleizes@univ-tlse3.fr; Carol Saunders, csaunders@cmh.edu

¶ SL, MFOD and SCS should be considered joint first author

& CJS and PEG should be considered joint senior author

¤a **Current address**: SUNY Upstate Medical University, Syracuse, NY, USA

¤b **Current address**: Division of Medical Genetics and Genomics, Stead Family University of Iowa Children's Hospital, The University of Iowa Carver College of Medicine, Iowa City, IA, USA

Grant numbers: Agence Nationale de la Recherche (anr.fr, France): grant #ANR-15-CE12-0001-02 (DBA Multigenes), grant #ANR-15-RAR3-0007-04 and grant #ANR-19-RAR4-0016

ABSTRACT

Diamond-Blackfan anemia is a rare genetic disease characterized by erythroblastopenia and a large spectrum of developmental anomalies. The vast majority of the cases genetically described are linked to heterozygous pathogenic variants in more than 20 ribosomal protein genes. Here we report an atypical clinical case of DBA associated with a missense variant in *RPL8*, which encodes RPL8/uL2, a protein of the 60S large ribosomal subunit. *RPL8* has been previously implicated as a candidate disease gene in one patient with DBA bearing another type of missense variant; however, evidence for pathogenicity was limited to computational tools. Using functional studies in lymphoblastoid cells as well as yeast models, we show that the *RPL8* variants detected in these two patients encode functionally deficient proteins that affect ribosome production and are therefore likely pathogenic. We propose to include *RPL8* in the list of DBA-associated genes.

KEYWORDS

Ribosomopathy, Diamond-Blackfan anemia, ribosomal protein, pre-ribosomal RNA, atypical case.

INTRODUCTION

Diamond-Blackfan Anemia (DBA) is a rare macrocytic anemia that usually presents during the first year of life (Da Costa et al., 2020; Lipton & Ellis, 2009). Approximately half of all patients present with congenital anomalies, including hypertelorism, flat nasal bridge, orofacial clefting, growth retardation, cardiac malformations, elevated fetal hemoglobin (HbF), and elevated erythrocyte

adenosine deaminase (eADA) enzyme activity. Another 20-30% have congenital urinary system malformations and skeletal abnormalities, including triphalangeal thumbs (Dooijeweert et al., 2018; Lipton & Ellis, 2009). Neoplasm occurrence in DBA patients is high, with increased risks to myelodysplastic syndrome (MDS), colon adenocarcinoma, osteosarcoma, and acute myeloid leukemia (AML). The cumulative incidence of developing a malignancy by age 46 is 20%, and median survival is 56 years (Vlachos et al., 2012).

Variable expressivity and incomplete penetrance contribute to the difficulties diagnosing DBA. Historically, a diagnosis has relied on multiple criteria, including anemia with normal or slight neutropenia in a child younger than 1 year, variable platelet counts, macrocytosis, normocellular bone marrow with a paucity of erythroid precursors, and reticulocytopenia (Dooijeweert et al., 2018; Lipton & Ellis, 2009; Ruggero & Shimamura, 2014; Vlachos & Muir, 2010). Elevated HbF and eADA are commonly observed in syndromes of bone marrow failure. These are non-specific but supportive in establishing a DBA diagnosis (Dooijeweert et al., 2018; Lipton & Ellis, 2009). Other considerations, such as Pearson syndrome, parvovirus B19, human immunodeficiency virus (HIV) and other infections should be ruled out prior to establishing a diagnosis of DBA (Farrar et al., 2008).

Increased knowledge of DBA epidemiology and the availability of clinical exome sequencing has led to improved diagnosis for DBA. In addition, the gene discovery rate has expanded exponentially (Ulirsch et al., 2018). To date, over 20 genes have been associated with DBA, with all but two of them encoding

proteins of the small or large ribosomal subunits (RPSs, RPLs, respectively): *RPS19, RPL5, RPL11, RPS26, RPL35A, RPS10, RPS17, RPS24, RPS7, RPS15A, RPS20, RPS27, RPS28, RPS29, RPL9, RPL15, RPL18, RPL26, RPL27, RPL31, RPL35* (Aubert et al., 2018; Bhar et al., 2020; Doherty et al., 2010; Draptchinskaia et al., 1999; Farrar et al., 2008, 2014; Gazda et al., 2006, 2008; Ikeda et al., 2017; Landowski et al., 2013; Lezzerini et al., 2020; Mirabello et al., 2014, 2017; Sankaran et al., 2012; Wang et al., 2015). The first eight genes together comprise roughly 50% of DBA cases. The most common contributor is *RPS19*, which is responsible for roughly 25% of cases (Da Costa et al., 2018; Ulirsch et al., 2018). The remaining genes are rare causes of DBA, described in 5 or fewer families. The two non-ribosomal genes encode the hematopoietic transcription factor GATA1 (Abdulhay et al., 2019; Klar et al., 2014; Ludwig et al., 2014; Parrella et al., 2014; Sankaran et al., 2012), and TSR2, a chaperone of RPS26 (Gripp et al., 2014); these two genes are X-linked and rarely associated with DBA or DBA-like disease. An estimated 45% of cases are inherited in an autosomal dominant fashion, while the remaining result from *de novo* changes or are X-linked (Da Costa et al., 2020).

Despite this impressive genetic heterogeneity, the list of DBA-associated ribosomal protein genes genes is restricted to those encoding essential ribosomal proteins, which primarily affect ribosome production (Aubert et al., 2018; Ellis & Gleizes, 2011). This suggests that any ribosomal protein encoding gene or gene regulating ribosomal biogenesis may be considered a DBA candidate gene. One such candidate, *RPL8*, encodes the RPL8/uL2 protein

constitutive of the 60S large ribosomal subunit. *RPL8* is highly constrained in the population for loss of function variants (gnomad.broadinstitute.org), suggesting haploinsufficiency is not tolerated in the general population. To date, genetic evidence for disease causality is limited to a single report of a girl with anemia but no dysmorphic features, whose exome sequencing identified a *de novo RPL8* variant, c.413C>T (p.Ser138Phe) (Wang et al., 2015) (Patient 91, Table 1). This variant was predicted to be deleterious by *in silico* algorithms but further evidence was not provided.

Here we report a second patient with a *de novo RPL8* variant, c.113A>G (p.His38Arg), presenting with a DBA-like phenotype. In addition, we use cellular and yeast models to demonstrate a partial loss of function for both variants, furthering the candidacy of *RPL8* as a DBA-associated gene.

MATERIALS AND METHODS

Cell culture and transfection

B-cell lymphocytes were separated from whole blood and transformed with EBV according to standard procedures. The lymphoblastoid cell lines (LCLs) thus obtained were cultured in RPMI-1640, while HeLa cells were grown in DMEM. These cell culture media were supplemented with 10% fetal bovine serum (FBS) and 1 mM sodium pyruvate (Gibco). Two 21-mer siRNAs (Eurogentec) were used to knock down expression of human *RPL8* mRNAs in HeLa cells: 5'-CCACAAAUAUAAGGCAAAGdTdT-3' (siRPL8-1), and 5'-AGACUGUGCAGGAGAAAGAdTdT-3' (siRPL8-2). The cell suspension (10×10^6

cells in Na phosphate buffer, pH 7.25, 250 mM sucrose, 1 mM $MgCl_2$), to which 10 µL of the siRNA solution (100 µM) were added, was transferred to an ice cold electroporation cuvette 4-mm in width (Bio-Rad). Electro-transformation was performed with square pulses at 240 V with a Gene Pulser (Bio-Rad). A scramble siRNA (siRNA-negative control duplex; Eurogentec) was used as a negative control. Cells were then plated in DMEM containing FBS and grown at 37°C for 48 h. Depletion of the *RPL8* mRNA was assessed by RT-qPCR using two sets of primers: 5'-CATCAAGGGCATCGTCAAGG-3' (RPL8_P1_Fwd) and 5'-CCTTCTTGCCGCAATACACA-3' (RPL8_P1_Rev); 5'-CCGTTATCTCCCACAACCCT-3' (RPL8_P2_Fwd) and 5'-GTTTGTCAATTCGGCCACCT-3' (RPL8_P2_Rev). The HPRT1 mRNA was used as a reference and amplified with primers 5'-AGCCCTGGCGTCGTGATTAG-3' (HPRT1-Fwd) and 5'-GTGATGGCCTCCCATCTCCT-3' (HPRT1-Rev).

Yeast strain, plasmids and media.

To test the effect of the absence of endogenous copy of uL2 protein we used the TY965 strain that only possesses one copy of *RPL2A* gene (YFR031c) under the control of GAL promoter and was kindly provided by Philip Milkereit (Pöll et al., 2009). The TY965 strain (his3-1, leu2-0, ura3-0, YIL018w::KANMX4/YFR031c-a::HIS3MX6) was then transformed with plasmids either expressing a wild-type copy of the *RPL2A* gene under its own promoter (pJD0629, a gift from Jonathan Dinman) (Meskauskas et al., 2008) or specific mutants obtained through site-directed PCR mutagenesis of pJD0629 with the following oligonucleotides (Eurogentec): RPL2_H38R_O1

(GGACTATGCTGAACGTCGTGGTTACATCCGTGGTATCGTT),

RPL2_H38R_O2

(AACGATACCACGGATGTAACCACGACGTTCAGCATAGTCC),

RPL2_V49D_O1

(GGTATCGTTAAGCAAATTGACCACGACTCCGGTAGAGGTG),

RPL2_V49D_O2

(CACCTCTACCGGAGTCGTGGTCAATTTGCTTAACGATACC),

RPL2_G138F_O1

(AACTACGTTATCATCATTTTCCACAACCCAGATGAAAACA),

(RPL2_G138F_O2

TGTTTTCATCTGGGTTGTGGAAAATGATGATAACGTAGTT).

Strains were grown in YNB minimum medium without uracil (yeast nitrogen base, Sigma) complemented with 2% glucose (Glu) or 2% galactose/1% sucrose (Gal/Suc) when indicated.

Growth analysis in yeast

Dilution spot assays were used to qualitatively monitor cell growth. For all conditions, yeast cells in logarithmic growth phase were diluted to OD_{600} = 0.5 in YNB medium. Subsequently, 10-fold serial dilutions of each strain were spotted onto YP-agarose plates containing glucose.

Growth at 30° C was also evaluated in liquid culture. Pre-cultures were grown overnight in YNB Gal/Suc. Then, 5 mL of culture at OD_{600} = 0.5 were washed twice in YNB without sugar and diluted in 10 mL of YP Glucose at OD_{600} = 0.1.

After 2 hours of recovery in the medium, the optical density was measured every 2 h during 8 h. Three independent clones were tested and the three readings were averaged for each time point. Doubling time was then estimated taking into account time points between 2 h and 6 h.

Isolation of RNAs from human cells and analysis by northern blot

For total RNA isolation, 15-20 × 10^6 cells were collected by centrifugation at 300 g, rinsed with cold PBS and lysed in 1-mL Tri reagent (Molecular Research Center, Inc.). After a first extraction with chloroform according to the manufacturer's instructions, the aqueous phase was further extracted with phenol-chloroform-isoamylic alcohol (25:24:1; Sigma), then with chloroform. Total RNAs were recovered after precipitation with 2-propanol. For northern blot analyses, RNAs were dissolved in formamide, denatured for 10 min at 70°C and separated on a 1.1% agarose gel containing 1.2% formaldehyde and 30 mM triethanolamine, 30 mM tricine, pH 7.9 (3 µg total RNAs/lane). RNAs were transferred to a Hybond N^+ nylon membrane (GE Healthcare) by passive transfer. Analyses of 5.8S rRNAs were performed on 6% polyacrylamide gels (19:1) (Bio-Rad) in TBE buffer containing 7 M urea. RNAs were electro transferred to Hybond N^+ nylon membrane. After cross-linking under UV light, pre-hybridization was performed for 1-3 hours at 45°C in 6X SSC, 5X Denhardt's solution, 0.5% SDS, 0.9 µg/mL tRNA. The 5'-radiolabeled oligonucleotide probe was incubated overnight. After washing twice for 10 min in 2X SSC, 0.1% SDS and once in 1X SSC, 0.1% SDS, the membrane was exposed to a PhosphorImager screen. Radioactive signals were revealed using a Typhoon

Trio PhosphorImager (GE Healthcare) and quantified using the MultiGauge software. The probes used were: 5'ITS1 (5'-CCTCGCCCTCCGGGCTCCGTTAATGATC-3'), ITS1-5.8S (5'-CTAAGAGTCGTACGAGGTCG-3'), ITS2 (5'-CTGCGAGGGAACCCCCAGCCGCGCA-3' and 5'-GCGCGACGGCGGACGACACCGCGGCGTC-3'), 18S (5'-TTTACTTCCTCTAGATAGTCAAGTTCGACC-3'), 5.8S (5'-GTTCTTCATCGACGCACGAGC-3'), 28S (5'-CCCGTTCCCTTGGCTGTGGTTTCGCTAGATA-3'), 7SK (5'-CATGGAGCGGTGAGGGAGGA-3' and 5'-GTGTCTGGAGTCTTGGAAGC-3').

Polysome gradient analysis of human cells

Lymphoblastoid cells (or HeLa cells 48 h post-transfection) were treated for 10 min with 100 µg/mL cycloheximide (Sigma). After washing with PBS containing cycloheximide, cell pellets were mechanically disrupted with a Dounce homogenizer in 10 mM HEPES, pH 7.9, 1.5 mM $MgCl_2$, 10 mM KCl, 0.5 mM DTT, containing cycloheximide. The cytoplasmic fractions were recovered by centrifugation for 10 min at 1 000 g and at 4°C, and then clarified further by two successive centrifugations at 10,000 g. A volume corresponding to 1 mg total proteins was loaded on 10-50% (w/w) sucrose gradients, prepared with a Gradient Master former (BioComp Instruments). After centrifugation at 4°C and at 160,000 g for 105 min in a SW41 rotor (Optima L100XP ultracentrifuge; Beckman Coulter), the fractions were collected at $OD_{254\ nm}$ with a Foxy Jr. gradient collector (Teledyne Isco).

Isolation of RNAs from yeast and analysis by northern blot

RNA extraction during the nutrient shift was performed from 5 mL culture at each time point following the previously described procedure (Lebaron et al., 2005). Then, RNAs (3 µg/well, except for experiment comparing same amount of cells for which 3 ul of RNA extract was used without normalization) were separated on a 1% agarose gel prepared with Tri/Tri buffer (30 mM triethanolamine and 30 mM tricine, pH 7.9) containing 1.2% formaldehyde and run in Tri/Tri buffer at 140 V. RNAs were transferred to a Hybond N+ nylon membrane (GE Healthcare) and fixed by UV cross-linking. Membranes were pre-hybridized for 1 h at 42°C in 6× SSC, 5× Denhardt's solution, 0.5% SDS, and 0.9 µg/mL tRNA. The ^{32}P-labeled oligodeoxynucleotide probe was added and incubated overnight at 42°C. The probes used in this study were 20S.3 (5' TTAAGCGCAGGCCCGGCTGG 3'), rRNA2.1 (5' GGCCAGCAATTTCAAGTTA 3'), 18S (5' CCGTCAGTGTAGCGCGCGTGCGGCCC3') and 25S (5'CTCACGACGGTCTAAACCC 3'). Labeled RNA signals were acquired with a PhosphorImager (GE Healthcare) and quantified with the Image Lab software.

Polysome gradient analysis on yeast

Yeast cells growing exponentially in YNB containing galactose or sucrose were washed twice with YNB and then shifted into YNB containing Glucose for 5 hours to reach an OD_{600} around 0.5. Then, 50 mg/mL cycloheximide (Sigma) was added directly to the culture medium. Cells were collected by centrifugation, rinsed with buffer K (20 mM Tris-HCl, pH 7.4, 50 mM KCl, 10 mM $MgCl_2$) supplemented with 50 mg/mL cycloheximide and collected again by

centrifugation. Dry pellets were resuspended with approximately one volume of ice-cold buffer K supplemented with 1 mM DTT, 1 tablet of complete EDTA-free protease inhibitor cocktail (Roche), 0.1 U/µL RNasin (Promega) and 50 mg/mL cycloheximide. About 250 µL of ice-cold glass beads (Sigma) were added to 500 µL aliquots of the resuspended cells and cells were broken by vigorous shaking, three times 2 min, separated by 2 min incubations on ice. Extracts were clarified through two successive centrifugations at 21,000 g and 4°C for 5 min and quantified by measuring absorbance at 260 nm. About 30 A260 units were loaded onto 10–50% sucrose gradients in buffer K, and then centrifuged for 150 min at 188,000 g and 4℃ in an Optima L-100XP Ultracentrifuge (Beckman-Coulter) using a SW41Ti rotor without brake. Following centrifugation, 18 fractions of 500 mL each were collected from the top of the gradients with a Foxy Jr. apparatus (Teledyne ISCO). The absorbance at 254 nm was measured during collection with a UA-6 device (Teledyne ISCO).

Ethical considerations

This study was approved by the institutional review board at Children's Mercy–Kansas City, Study #11120514. Parents provided written informed consent.

RESULTS

Clinical Report

The patient was the fourth child born to non-consanguineous parents when her mother was 33 years old, and her father 53. She was her mother's

eleventh pregnancy, having had three miscarriages from multiple relationships. The pregnancy was complicated by an intracardiac echogenic focus, intrauterine growth restriction, and reduced fetal movements. Induced vaginal delivery occurred at 37 weeks of gestation. At birth she weighed 6 pounds 3 ounces, and measured 19 inches in length. Her medical history was otherwise unremarkable until seven months of age, when a transient pupil asymmetry was noted. At eight months of age, she was evaluated for failure to thrive, inadequate caloric intake and constipation. At nine months, she was seen in the genetics clinic for failure to thrive, relative microcephaly, and bilateral triphalangeal thumbs. Upon examination her height was 63.7 cm (0.16 centile, WHO), weight was 6.93 kg (5.82 centile, WHO), and head circumference was 41.75 cm (approximately 5th centile, WHO). She sat independently, but had slightly reduced central tone. Apart from having slight telecanthus, she was otherwise non-dysmorphic. The transient pupil asymmetry previously noted was also documented at this time. Negative etiological studies included chromosome analysis, array-CGH, and chromosome breakage studies. Diamond-Blackfan anemia was considered, but complete blood count (CBC) showed only mildly elevated white cell counts (26.21 X 10^3, range: 6.00-17.50) and platelets (535 x 10^3, range: 150-450), with normal hemoglobin but slight macrocytosis (mean cell volume 91.3 fL; range 70.0-86.0fL) in the presence of slightly reduced mean corpuscular hemoglobin concentration (31.2gm/dL; range 31.5-36.5)

Clinical trio exome sequencing was performed by an external reference laboratory, GeneDx, Gaithersburg, MD. Only one variant was reported, a

heterozygous *de novo* missense variant in *RPL8*, c.113A>G (p.His38Arg) (NM_001317782.2:n.374A>G). This variant is absent in population datasets (gnomAD and ExAC of the Broad Institute). Though the lack of established gene-disease relationship resulted in the variant being categorized as one of uncertain significance, the patient was seen by hematology at 14 months of age for follow up of this result, where she was noted to have symptoms of fatigue, but a normal CBC. At age 19 months she was again seen in the hematology clinic for continued monitoring and was found to be slightly anemic (hemoglobin of 11.2 g/dL, range: 12.0-16.0), with mild leukocytosis (WBC of 19.11 x 10^3, range: 6.00-17.50) and normal platelets. Her MCV (82.8 fL, range: 70.0-86.0) and reticulocyte counts were also normal. The anemia resolved without treatment, and subsequent blood counts were normal. A bone marrow examination was not performed. There was no evidence of hepatosplenomegaly or pancreatic insufficiency. Fetal hemoglobin and ADA testing was requested but not performed. She continues to be followed in the endocrine clinic for growth issues: height Z score -1.59, weight -0.79, with linear growth improving at the age of 4 and a half.

Cells expressing the *RPL8* p.H38R variant display a deficit in 60S ribosomal subunits

To assess the functional impact of the *RPL8* p.H38R missense variant on ribosome synthesis, we examined the processing of the precursors to the 18S, 28S and 5.8S rRNAs in EBV-transformed lymphocytes established from the patient. The ribosomal RNA processing intermediates (pre-rRNAs) were detected

by northern blot with probes directed against the external and internal transcribed spacers that flank the mature RNA sequences (Supp. Fig. S1). Changes in the pre-rRNA pattern may reveal defects in the cleavage kinetics provoked by a pathological variant (Choesmel et al., 2007; Da Costa et al., 2018; Farrar et al., 2014).

As a reference, we examined HeLa cells depleted of RPL8/uL2 upon treatment with siRNAs. Knockdown of RPL8/uL2 synthesis led to the strong accumulation of 32S pre-rRNA and the parallel reduction of its processing products, the 12S pre-rRNA (Fig. 1A). We consistently observed a decrease in the 28S/18S rRNA ratio, indicating that this RPL is essential in human cells for production of the large ribosomal subunit (Fig. 1, A-B). This was confirmed by analysis of cytoplasmic ribosomes on sucrose gradient, which showed a marked decrease of the free 60S subunits peak, impairment of monosome (80S) and polysome formation, and presence of halfmers indicative of a lack of 60S particles (Fig. 1C). A slight accumulation of 18S-E pre-rRNA relative to 21S (Fig. 1A) suggested that synthesis of the 40S subunit was also slightly affected (Fig. 1A), which is not unusual for a dysfunctional 60S subunit pathway.

Total RNAs extracted from a lymphoblastoid cell line (LCL) derived from the patient blood sample exhibited a mild difference in the pre-rRNA pattern when compared to those of her parents (Fig. 2A-B). Unlike in RPL8/uL2 depleted cells, the 32S pre-rRNA level was slightly reduced relative to one of its precursors, the 41S pre-rRNA. The patient pre-rRNA pattern was characterized by a slight accumulation of 41S and 21S pre-rRNAs relative to the precursors,

suggesting a delay in cleavage of the ITS1 at sites 2 and E. Neither the patterns of the 5.8S precursors (5.8S-ITS2 probe), nor the levels of 5.8S rRNA were significantly affected in the patient's LCL relative to the parents' (Fig. 2C). These data suggest that pre-rRNA processing is moderately affected in this patient, but not in a way expected for *RPL8* haploinsufficiency, since the LCL does not phenocopy *RPL8* depleted cells. When total extracts from the different LCLs were fractionated by ultracentrifugation on sucrose gradients and polysome profiles were analyzed by optical density, the polysome profiles obtained with the patient LCL extracts showed a clear reduction of the free 60S subunit peak relative to the free 40S subunit peak, indicating that production or stability of the large subunit is impaired in the patient cells (Fig. 2D).

Expression of uL2 p.H38R and p.G138F mutants in yeast affect cell growth

To model the effects of the patient's variant in a context devoid of wild-type uL2, we employed yeast *S. cerevisiae,* in which uL2 is encoded by two paralogues highly homologous to human RPL8 with the identical amino acid (histidine) at position 38 (Fig. 3A). uL2 in yeast is essential for 60S subunit biogenesis and cell viability (Lucioli et al., 1988; Poll et al., 2009). We also took advantage of this system to assess the functional impact of the previously reported p.S138F variant in a DBA patient (Wang et al., 2015). While serine 138 in human uL2 is replaced in yeast uL2 by a glycine (G138), both amino acids are relatively small and uncharged, and are qualified as mildly conserved by the PRALINE alignment software (Fig. 3A). Noticeably, they are positioned in a highly conserved segment of the protein (Fig. 3A), which is likely to be similarly

affected by the presence of a phenylalanine at position 138 in yeast and human uL2.

To test the effect of substitutions equivalent to human p.H38R and p.S138F on uL2 function in yeast, we used a previously described strain that possesses a single copy of *RPL2* (orthologous to human *RPL8*) under control of the conditional *GAL* promoter, which is repressed in the presence of glucose (Pöll et al., 2009). We transformed this strain with plasmids supporting constitutive expression of either the wild-type uL2 (uL2 WT), the patient-related mutants p.H38R and p.G138F, or a previously described translationally deficient mutant p.V49D as a control (Meskauskas et al., 2008). We set out a drop-test analysis to examine the ability of the uL2 variants to support cell growth (Fig. 3B). Upon repression of the genomic *RPL2* in the presence of glucose on rich YP medium, viability was fully rescued by expression of the wild-type uL2 from the plasmid (Fig. 3B). The p.V49D mutant only partially complemented growth in glucose medium with fewer and smaller colonies observed, confirming previous observations (Meskauskas et al., 2008). The uL2 p.G138F mutant displayed fewer colonies than with the wild-type construct in the strongest dilutions. Expression of the uL2 p.H38R mutant also led to a lower number of colonies observed in the most diluted drops. A similar trend was observed on synthetic medium containing glucose (Supp. Fig. S2, panel A). Of note, when grown on synthetic medium in the presence of galactose and sucrose (which allows expression of *RPL2* on the genome), the strains expressing the p.V49D and p.G138F mutants showed a growth defect (visible at the highest cell dilution),

suggesting a dominant-negative effect of these variants over the wild-type uL2 (Supp. Fig. S2, panel A).

To refine the analysis, we measured the growth rate of these strains in liquid medium (Fig. 3C). As shown in Figure 3C in rich YP medium, the uL2 mutants supported growth in glucose, but the doubling time shifted from 1 h 49 min for wild-type uL2, to 2 h 06 min for uL2 p.H38R, 2 h 36 min for uL2 p.G138F and 2 h 51 min for uL2 p.V49D. Substitution p.V49D, which was proposed to impede translation (Meskauskas et al., 2008), affected cell growth most strongly. The effect observed with uL2 p.H38R in liquid culture was mild, but highly reproducible and statistically significant, while the p.G138F mutant showed a more pronounced growth defect. The impact of the mutations was similar when yeasts were grown in synthetic medium (Supp. Fig. 2, panel B). These results indicate that the uL2 variants found in the two patients are hypomorphic variants that integrate into 60S ribosomal particles but are less functional than the wild-type protein.

The uL2 p.H38R and p.G138F mutants affect pre-ribosomal RNA processing in yeast

We next analyzed the effect of the uL2 variants on pre-rRNA maturation in yeast. Depletion of uL2 in yeast was previously shown to delay early processing of the 35S and 27SA precursors and to cause accumulation of the 7S pre-rRNA, a precursor to the 5.8S rRNA (Pöll et al., 2009). Pre-rRNA processing was assessed by northern blot in the strains described above cultured in presence of galactose or glucose (Fig. 4A). The ratios between all pre-rRNA intermediates

were quantified relative to wild-type uL2 expressing cells (Fig. 4B). Interestingly, the strains expressing the uL2 p.G138F and p.V49D mutants already accumulated 35S or 7S pre-rRNAs in galactose containing medium when compared to wild-type uL2 (Fig. 4 A-B), indicating a dominant-negative effect of these mutations. When expression of the chromosomal *RPL2* gene was repressed with glucose, the 35S, 27SA and 7S pre-rRNAs strongly accumulated in the strain carrying the empty vector (Fig. 4A-B). These defects were fully rescued in cells expressing wild-type uL2 from a plasmid. In contrast, the p.V49D mutant exhibited severe accumulation of the 35S, 27SA and 7S pre-rRNAs. Processing was less affected in cells expressing the patients-related variants p.H38R and p.G138F, but a clear accumulation of 7S pre-rRNA was also observed with both (Fig. 4B), indicating impaired 3'-end maturation of this precursor by the exosome (Poll et al., 2009). Accumulation of 35S pre-RNA was not observed with these mutations, suggesting that they only affect one of two distinct pre-rRNA processing events for which yeast uL2 is required. Consistent with a defect in formation of the large subunit, the 25S/18S ratio decreased with the three uL2 mutations. This was further evidenced by the analysis of the 25S and 18S rRNA content from a similar number of cells by gel electrophoresis and ethidium bromide staining (Fig. 4C). The three uL2 mutations reproducibly impeded 18S and 25S rRNAs production to various degrees, including the uL2 p.H38R variant.

When cell extracts were fractionated on sucrose gradients, polysome profiles displayed a major deficit of 60S subunits in yeast depleted of uL2 (Fig.

5A). The ratio of free 60S over free 40S subunits dropped by 60% when compared to control (Fig. 5A-B), and polysomes showed the presence of halfmers, which result from a deficit of 60S ribosomal subunits relative to 40S subunits during translation initiation (Fig. 5A). This phenotype was fully rescued by exogenous expression of wild-type uL2. In contrast, the strain expressing the translationally deficient p.V49D mutant also exhibited a strong reduction of 60S subunits (free 60S/free 40S = 0.5) and the presence of halfmers (Fig. 5A). Along this line, cells expressing the uL2 p.H38R or p.G138F variants also showed a reproducible deficit of free 60S subunits relative to free 40S subunits. Halfmers were clearly visible as independent peaks in the polysome profile with the p.G138F variant, while shoulders in the polysome peaks also suggested their occurrence in yeast expressing the p.H38R variant.

Overall, these results indicate that the p.H38R and p.G138F mutations partially impair yeast uL2 function in the processing of the large ribosomal subunit RNAs and support a pathogenic role of the p.S138F and p.H38R variants of *RPL8* in patients.

Different impacts of the p.H38R and p.S138F variants on RPL8 structure

We next examined the potential impact of the p.H38R and p.S138F variants on the structure of RPL8. Previous work has shown that DBA-linked substitutions in RPS19 either destabilize the protein by disrupting some intramolecular bond, or prevent incorporation of the protein in nascent ribosomal subunits by changing amino acids that interact with the ribosomal RNA. Both situations lead to haploinsufficiency of the protein (Angelini et al., 2007; Crétien

et al., 2008; Gregory et al., 2007). Our results in yeast indicate that the RPL8 variants can incorporate into pre-60S particles, but the deficit in 60S subunit levels observed with both of them suggests that incorporation is suboptimal, especially with the p.G138F substitution. The structure of the variants in the human ribosome was modeled using Phyre2 based on a recent structure solved by cryo-electron microscopy (Fig. 6). As shown in Fig. 6C, substitution of histidine 38 by an arginine changed the conformation of an helix; the arginine potentially establishes new bonds with the neighboring guanosine 4115 in the 28S rRNA and with isoleucine 41 in protein RPL7A. Changing serine 138 by a phenylalanine did not directly affect RPL8 interaction with neighboring molecules in the ribosome, but introduced new possible bonds with isoleucine 137 and positioned the aromatic ring of phenylalanine in close proximity to arginine 147. While this may not be drastic in the context of the ribosome, such a change with a bulky amino acid may impact the folding of the protein and lead to its degradation upstream of its incorporation into the ribosomes. These analyses were supported by similar modeling performed on the yeast ribosome (Fig. 6D). The p.H38R and p.G138F substitutions yielded very similar effects on the structure. We also assessed the mutation of valine 49 to aspartic acid in yeast uL2 that we used here as control (Fig. 6D). Similar to the p.G138F variant, this substitution appears to affect intramolecular rather than intermolecular interactions in the ribosome, which is also the case for the p.I49D substitution in the human protein (Fig. 6C).

DISCUSSION

We present evidence that DBA can be caused by variants in *RPL8*, the gene encoding RPL8/uL2 ribosomal protein. Our analysis shows that the rare *RPL8* variant, c.413C>T (p.S138F), previously reported in a DBA patient (Wang et al., 2015) encodes a partially dysfunctional ribosomal protein, which perturbs pre-rRNA processing and production of 60S ribosomal subunits as observed with other DBA associated RP genes. In addition, we report a second *RPL8* hypomorphic variant in a patient presenting a DBA-like phenotype, but with no bone marrow failure. This variant also affects the function of the protein and 60S subunit production, albeit more modestly than the variant identified in the *bona fide* DBA patient.

Using yeast *S. cerevisiae*, we directly assessed the functional impact of these variants in strains in which expression of the wild-type allele could be repressed. Indeed, expression of either of the two variants upon shutdown of the wild-type gene affected ribosome production in yeast, as attested both by the accumulation of precursors to the 60S subunit RNAs and by the deficit of 60S subunits in ribosome profiles. The two substitutions do not fully abrogate the capacity of uL2 to sustain viability in yeast, which indicates that these uL2 variants are hypomorphic and integrate into the 60S ribosomal subunit. Similar observations in yeast with DBA-linked *RPS19* variants were previously reported (Gregory et al., 2007; Léger-Silvestre et al., 2005). The deficit in 60S subunits that we observed in yeast only expressing the p.G138F variant indicates that pre-60S subunit maturation is deficient. Modeling results in Fig. 6 indicate that substitution of serine 138 by a bulky hydrophobic amino acid (phenylalanine) in

human RPL8/uL2 may not affect significantly its interaction with the ribosome, but generate aberrant intramolecular hydrophobic interactions interfering with its folding. This could provoke the degradation of a fraction of the protein and result in RPL8/uL2 haploinsufficiency, as previously demonstrated for DBA-linked RPS19 variants (Angelini et al., 2007; Crétien et al., 2008; Gregory et al., 2007). However, the related p.G138F substitution in yeast uL2 has a dominant-negative effect on cell growth (Supp. Fig. 2, panel A) and pre-rRNA processing (Fig. 4A,B), which suggests that this mutated form can compete with the wild-type uL2 for incorporation into pre-ribosomes. This effect could also contribute to the pathogenicity of the p.S138F variant. We conclude that expression of the p.S138F variant in the DBA patient reported in a Japanese cohort (Wang et al., 2015) affects ribosome synthesis and results in a deficit of functional ribosomes, similar to other DBA variants of ribosomal protein genes. These observations establish *RPL8* as a new gene involved in DBA.

The p.H38R substitution had a milder effect on ribosome production and cell growth in yeast than the p.G138F mutation, and perturbation of pre-rRNA processing was limited to a defect in 7S pre-rRNA maturation in yeast (Fig. 4 A-B). Similarly, lymphoblastoid cells from the patient identified here showed a deficit in free 60S subunit in polysome profiles, but with no clear accumulation of the 32S pre-rRNA, the precursor to the rRNAs of the 60S subunit. The impact on cell growth and 60S subunit accumulation observed in yeast strongly suggests however that the human p.H38R variant is indeed a hypomorphic form of uL2. The milder impact of this variant on ribosome synthesis correlates with the

degree of regional constraint observed for missense variants in *RPL8*; histidine 38 lies in a moderately constrained region in terms of missense tolerance as opposed to serine 138, which is in a region highly intolerant to missense variants (Supp. Fig. 3). According to the modeling results, presence of the negatively-charged aspartic acid at position 38 instead of a positively charged histidine can lead to new interactions with the 28S rRNA and ribosomal protein RPL7A. This may alter the kinetics of RPL8 incorporation into the pre-60S particles, or influence the mechanics of translation. However, the limited deficit of 60S particles indicates that this missense variant does not strongly destabilize uL2/RPL8.

The variable features observed in the two *RPL8* patients may simply relate to the variable phenotype expression commonly seen for DBA, even within the same family. While the laboratory values in our patient are very mild and transient, they are of interest in the presence of thumb anomalies and short stature; such mild presentations are well documented in association with DBA. Thumb anomalies are sometimes the only or main finding and in the presence of mild anemia with no macrocytosis may result in a delayed diagnosis (Steinberg-Shemer et al., 2016). Some patients are diagnosed later in life with a mild anemia requiring no therapy (Gazda et al., 2008). In addition, familial studies of patients with DBA often reveal substantial intrafamilial variability—ranging from “silent carriers” to transfusion dependence in a single family in individuals with the same variant. In such families, some otherwise healthy individuals may show only macrocytosis and/or isolated elevation of eADA as the only finding (Willig et

al., 1999). Such variable expression may explain why the p.H38R patient only exhibits thumb anomalies and mild anemia or even subclinical findings. Indeed, one study on the common non-anemia findings in *RPL11*-related DBA found that 51% (27/53) of affected individuals exhibit thumb anomalies, indicating this is a common, albeit nonspecific, sign in DBA (Carlston et al., 2017). Alternatively, we may speculate that the pathogenic mechanisms affecting erythropoiesis and skeletal malformation in DBA might be uncoupled in the RPL8 p.H38R substitution. While erythropoiesis in DBA appears to be primarily sensitive to a quantitative deficit of functional ribosomes, which affects translation of the erythropoiesis master regulator GATA-1 (Khajuria et al., 2018), developmental defects could rather be caused by different mechanisms, like p53 activation by ribosomal stress or translation defects linked to changes in ribosome quality rather than quantity. Along this line, insertion and missense variants of ribosomal protein RPL13 that only mildly affect ribosome biogenesis and are present in translating ribosomes were recently unambiguously associated to bone development syndromes with no hematopoietic phenotype (Costantini et al., 2020; Le Caignec et al., 2019; Reinsch et al., 2020).

In conclusion, *RPL8* may be added to the long list of ribosomal protein genes associated with DBA. Reports of additional patients and further functional characterization are needed to understand this variable disease and the contribution of missense ribosomal protein gene variants to developmental anomalies.

ACKNOWLEDGMENTS

The authors are grateful to the family for their participation. They would like also to thank Julien Marcoux and Carine Froment (IPBS, CNRS, Toulouse, France) for their collaboration. PEG, MFOD, and SL were funded by the Agence Nationale de la Recherche (ANR, France) through the white program grant #ANR-15-CE12-0001-02 (DBA Multigenes), grant #ANR-15-RAR3-0007-04 (EuroDBA) under the frame of the E-Rare Eranet program and grant #ANR-19-RAR4-0016 (RiboEurope) under the frame of EJP RD programme JTC 2019. The authors have declared that no competing interests exist.

DATA AVAILABILITY STATEMENT

The data that support the findings of this study are available from the corresponding author upon reasonable request. The *RPL8* variant c.113A>G (p.His38Arg) (NM_001317782.2:n.374A>G) reported here has been submitted to ClinVar (https://www.ncbi.nlm.nih.gov/clinvar/) with ID number SUB10806262.

REFERENCES

Abdulhay, N. J., Fiorini, C., Verboon, J. M., Ludwig, L. S., Ulirsch, J. C., Zieger, B., Lareau, C. A., Mi, X., Roy, A., Obeng, E. A., Erlacher, M., Gupta, N., Gabriel, S. B., Ebert, B. L., Niemeyer, C. M., Khoriaty, R. N., Ancliff, P., Gazda, H. T., Wlodarski, M. W., & Sankaran, V. G. (2019). Impaired human hematopoiesis due to a cryptic intronic GATA1 splicing mutation. *Journal of Experimental Medicine*, *216*(5), 1050-1060. https://doi.org/10.1084/jem.20181625

Angelini, M., Cannata, S., Mercaldo, V., Gibello, L., Santoro, C., Dianzani, I., & Loreni, F. (2007). Missense mutations associated with Diamond-Blackfan anemia affect the assembly of ribosomal protein S19 into the ribosome. *Human Molecular Genetics*, *16*(14), 1720-1727. https://doi.org/10.1093/hmg/ddm120

Aubert, M., O'Donohue, M.-F., Lebaron, S., & Gleizes, P.-E. (2018). Pre-Ribosomal RNA Processing in Human Cells: From Mechanisms to Congenital Diseases. *Biomolecules*, *8*(4), 123. https://doi.org/10.3390/biom8040123

Bhar, S., Zhou, F., Reineke, L. C., Morris, D. K., Khincha, P. P., Giri, N., Mirabello, L., Bergstrom, K., Lemon, L. D., Williams, C. L., Toh, Y., Elghetany, M. T., Lloyd, R. E., Alter, B. P., Savage, S. A., & Bertuch, A. A. (2020). Expansion of germline RPS20

mutation phenotype to include Diamond–Blackfan anemia. *Human Mutation*, *41*(11), 1918-1930. https://doi.org/10.1002/humu.24092

Carlston, C. M., Afify, Z. A., Palumbos, J. C., Bagley, H., Barbagelata, C., Wooderchak-Donahue, W. L., Mao, R., & Carey, J. C. (2017). Variable expressivity and incomplete penetrance in a large family with non-classical Diamond-Blackfan anemia associated with ribosomal protein L11 splicing variant. *American Journal of Medical Genetics Part A*, *173*(10), 2622-2627. https://doi.org/10.1002/ajmg.a.38360

Choesmel, V., Bacqueville, D., Rouquette, J., Noaillac-Depeyre, J., Fribourg, S., Cretien, A., Leblanc, T., Tchernia, G., Da Costa, L., & Gleizes, P. E. (2007). Impaired ribosome biogenesis in Diamond-Blackfan anemia. *Blood*, *109*(3), 1275-1283. https://doi.org/10.1182/blood-2006-07-038372

Costantini, A., Alm, J. J., Tonelli, F., Valta, H., Huber, C., Tran, A. N., Daponte, V., Kirova, N., Kwon, Y.-U., Bae, J. Y., Chung, W. Y., Tan, S., Sznajer, Y., Nishimura, G., Näreoja, T., Warren, A. J., Cormier-Daire, V., Kim, O.-H., Forlino, A., … Mäkitie, O. (2020). Novel RPL13 Variants and Variable Clinical Expressivity in a Human Ribosomopathy With Spondyloepimetaphyseal Dysplasia. *Journal of Bone and Mineral Research: The Official Journal of the American Society for Bone and Mineral Research*. https://doi.org/10.1002/jbmr.4177

Crétien, A., Hurtaud, C., Moniz, H., Proust, A., Marie, I., Wagner-Ballon, O., Choesmel, V., Gleizes, P.-E., Leblanc, T., Delaunay, J., Tchernia, G., Mohandas, N., & Da Costa, L. (2008). Study of the effects of proteasome inhibitors on ribosomal protein S19 (RPS19) mutants, identified in patients with Diamond-Blackfan anemia. *Haematologica*, *93*(11), 1627-1634. https://doi.org/10.3324/haematol.13023

Da Costa, L., Leblanc, T., & Mohandas, N. (2020). Diamond-Blackfan anemia. *Blood*, *136*(11), 1262-1273. https://doi.org/10.1182/blood.2019000947

Da Costa, L., O'Donohue, M.-F., van Dooijeweert, B., Albrecht, K., Unal, S., Ramenghi, U., Leblanc, T., Dianzani, I., Tamary, H., Bartels, M., Gleizes, P.-E., Wlodarski, M., & MacInnes, A. W. (2018). Molecular approaches to diagnose Diamond-Blackfan anemia: The EuroDBA experience. *European Journal of Medical Genetics*, *61*(11), 664-673. https://doi.org/10.1016/j.ejmg.2017.10.017

Doherty, L., Sheen, M. R., Vlachos, A., Choesmel, V., O'Donohue, M. F., Clinton, C., Schneider, H. E., Sieff, C. A., Newburger, P. E., Ball, S. E., Niewiadomska, E., Matysiak, M., Glader, B., Arceci, R. J., Farrar, J. E., Atsidaftos, E., Lipton, J. M., Gleizes, P. E., & Gazda, H. T. (2010). Ribosomal protein genes RPS10 and RPS26 are commonly mutated in Diamond-Blackfan anemia. *Am J Hum Genet*, *86*(2), 222-228. https://doi.org/10.1016/j.ajhg.2009.12.015

Dooijeweert, B. van, Ommen, C. H. van, Smiers, F. J., Tamminga, R. Y. J., Loo, M. W. te, Donker, A. E., Peters, M., Granzen, B., Gille, H. J. J. P., Bierings, M. B., MacInnes, A. W., & Bartels, M. (2018). Pediatric Diamond-Blackfan anemia in the Netherlands: An overview of clinical characteristics and underlying molecular defects. *European Journal of Haematology*, *100*(2), 163-170. https://doi.org/10.1111/ejh.12995

Draptchinskaia, N., Gustavsson, P., Andersson, B., Pettersson, M., Willig, T. N., Dianzani, I., Ball, S., Tchernia, G., Klar, J., Matsson, H., Tentler, D., Mohandas, N.,

Carlsson, B., & Dahl, N. (1999). The gene encoding ribosomal protein S19 is mutated in Diamond- Blackfan anaemia. *Nature Genetics*, *21*(2), 169-175.

Ellis, S. R., & Gleizes, P.-E. (2011). Diamond Blackfan anemia: Ribosomal proteins going rogue. *Semin Hematol*, *48*, 89-96. https://doi.org/10.1053/j.seminhematol.2011.02.005

Farrar, J. E., Nater, M., Caywood, E., McDevitt, M. A., Kowalski, J., Takemoto, C. M., Talbot, C. C., Meltzer, P., Esposito, D., Beggs, A. H., Schneider, H. E., Grabowska, A., Ball, S. E., Niewiadomska, E., Sieff, C. A., Vlachos, A., Atsidaftos, E., Ellis, S. R., Lipton, J. M., … Arceci, R. J. (2008). Abnormalities of the large ribosomal subunit protein, Rpl35a, in Diamond-Blackfan anemia. *Blood*, *112*(5), 1582-1592. https://doi.org/10.1182/blood-2008-02-140012

Farrar, J. E., Quarello, P., Fisher, R., O'Brien, K. A., Aspesi, A., Parrella, S., Henson, A. L., Seidel, N. E., Atsidaftos, E., Prakash, S., Bari, S., Garelli, E., Arceci, R. J., Dianzani, I., Ramenghi, U., Vlachos, A., Lipton, J. M., Bodine, D. M., & Ellis, S. R. (2014). Exploiting pre-rRNA processing in Diamond Blackfan anemia gene discovery and diagnosis. *American Journal of Hematology*, *89*(10), 985-991. https://doi.org/10.1002/ajh.23807

Gazda, H. T., Grabowska, A., Merida-Long, L. B., Latawiec, E., Schneider, H. E., Lipton, J. M., Vlachos, A., Atsidaftos, E., Ball, S. E., Orfali, K. A., Niewiadomska, E., Da Costa, L., Tchernia, G., Niemeyer, C., Meerpohl, J. J., Stahl, J., Schratt, G., Glader, B., Backer, K., … Sieff, C. A. (2006). Ribosomal protein S24 gene is mutated in Diamond-Blackfan anemia. *American journal of human genetics*, *79*(6), 1110-1118. https://doi.org/10.1086/510020

Gazda, H. T., Sheen, M. R., Vlachos, A., Choesmel, V., O'Donohue, M. F., Schneider, H., Darras, N., Hasman, C., Sieff, C. A., Newburger, P. E., Ball, S. E., Niewiadomska, E., Matysiak, M., Zaucha, J. M., Glader, B., Niemeyer, C., Meerpohl, J. J., Atsidaftos, E., Lipton, J. M., … Beggs, A. H. (2008). Ribosomal protein L5 and L11 mutations are associated with cleft palate and abnormal thumbs in Diamond-Blackfan anemia patients. *Am J Hum Genet*, *83*(6), 769-780. https://doi.org/10.1016/j.ajhg.2008.11.004

Gregory, L. A., Aguissa-Touré, A.-H., Pinaud, N., Legrand, P., Gleizes, P.-E., & Fribourg, S. (2007). Molecular basis of Diamond-Blackfan anemia: Structure and function analysis of RPS19. *Nucleic Acids Research*, *35*(17), 5913-5921. https://doi.org/10.1093/nar/gkm626

Gripp, K. W., Curry, C., Olney, A. H., Sandoval, C., Fisher, J., Chong, J. X. L., Pilchman, L., Sahraoui, R., Stabley, D. L., & Sol-Church, K. (2014). Diamond-Blackfan anemia with mandibulofacial dystostosis is heterogeneous, including the novel DBA genes TSR2 and RPS28. *American Journal of Medical Genetics, Part A*, *164*(9), 2240-2249. https://doi.org/10.1002/ajmg.a.36633

Ikeda, F., Yoshida, K., Toki, T., Uechi, T., Ishida, S., Nakajima, Y., Sasahara, Y., Okuno, Y., Kanezaki, R., Terui, K., Kamio, T., Kobayashi, A., Fujita, T., Sato-Otsubo, A., Shiraishi, Y., Tanaka, H., Chiba, K., Muramatsu, H., Kanno, H., … Ito, E. (2017). Exome sequencing identified RPS15A as a novel causative gene for Diamond-

Blackfan anemia. *Haematologica*, *102*(3), e93-e96. https://doi.org/10.3324/haematol.2016.153932

Khajuria, R. K., Munschauer, M., Ulirsch, J. C., Fiorini, C., Ludwig, L. S., McFarland, S. K., Abdulhay, N. J., Specht, H., Keshishian, H., Mani, D. R., Jovanovic, M., Ellis, S. R., Fulco, C. P., Engreitz, J. M., Schütz, S., Lian, J., Gripp, K. W., Weinberg, O. K., Pinkus, G. S., … Sankaran, V. G. (2018). Ribosome Levels Selectively Regulate Translation and Lineage Commitment in Human Hematopoiesis. *Cell*, *173*(1), 90-103.e19. https://doi.org/10.1016/j.cell.2018.02.036

Klar, J., Khalfallah, A., Arzoo, P. S., Gazda, H. T., & Dahl, N. (2014). Recurrent GATA1 mutations in Diamond-Blackfan anaemia. *British Journal of Haematology*, *166*(6), 949-951. https://doi.org/10.1111/bjh.12919

Landowski, M., O'Donohue, M. F., Buros, C., Ghazvinian, R., Montel-Lehry, N., Vlachos, A., Sieff, C. A., Newburger, P. E., Niewiadomska, E., Matysiak, M., Glader, B., Atsidaftos, E., Lipton, J. M., Beggs, A. H., Gleizes, P. E., & Gazda, H. T. (2013). Novel deletion of RPL15 identified by array-comparative genomic hybridization in Diamond-Blackfan anemia. *Hum Genet*, *132*(11), 1265-1274. https://doi.org/10.1007/s00439-013-1326-z

Le Caignec, C., Ory, B., Lamoureux, F., O'Donohue, M.-F., Orgebin, E., Lindenbaum, P., Téletchéa, S., Saby, M., Hurst, A., Nelson, K., Gilbert, S. R., Wilnai, Y., Zeitlin, L., Segev, E., Tesfaye, R., Nizon, M., Cogne, B., Bezieau, S., Geoffroy, L., … Isidor, B. (2019). Novel RPL13 variants and variable clinical expressivity in a human ribosomopathy with spondyloepimetaphyseal dysplasia. *American Journal of Human Genetics*, *105*(5), 1040-1047. https://doi.org/10.1016/j.ajhg.2019.09.024

Lebaron, S., Froment, C., Fromont-Racine, M., Rain, J.-C., Monsarrat, B., Caizergues-Ferrer, M., & Henry, Y. (2005). The Splicing ATPase Prp43p Is a Component of Multiple Preribosomal Particles. *Molecular and Cellular Biology*, *25*(21), 9269-9282. https://doi.org/10.1128/MCB.25.21.9269-9282.2005

Léger-Silvestre, I., Caffrey, J. M., Dawaliby, R., Alvarez-Arias, D. A., Gas, N., Bertolone, S. J., Gleizes, P.-E., & Ellis, S. R. (2005). Specific Role for Yeast Homologs of the Diamond Blackfan Anemia-associated Rps19 Protein in Ribosome Synthesis. *Journal of Biological Chemistry*, *280*(46), 38177-38185. https://doi.org/10.1074/jbc.M506916200

Lezzerini, M., Penzo, M., O'Donohue, M.-F., Marques dos Santos Vieira, C., Saby, M., Elfrink, H. L., Diets, I. J., Hesse, A.-M., Couté, Y., Gastou, M., Nin-Velez, A., Nikkels, P. G. J., Olson, A. N., Zonneveld-Huijssoon, E., Jongmans, M. C. J., Zhang, G., van Weeghel, M., Houtkooper, R. H., Wlodarski, M. W., … MacInnes, A. W. (2020). Ribosomal protein gene RPL9 variants can differentially impair ribosome function and cellular metabolism. *Nucleic Acids Research*, *48*(2), 770. https://doi.org/10.1093/nar/gkz1042

Lipton, J. M., & Ellis, S. R. (2009). Diamond-Blackfan Anemia: Diagnosis, Treatment, and Molecular Pathogenesis. *Hematology/Oncology Clinics of North America*, *23*(2), 261-282. https://doi.org/10.1016/j.hoc.2009.01.004

Lucioli, A., Presutti, C., Ciafrè, S., Caffarelli, E., Fragapane, P., & Bozzoni, I. (1988). Gene dosage alteration of L2 ribosomal protein genes in Saccharomyces

cerevisiae: Effects on ribosome synthesis. *Molecular and Cellular Biology*, *8*(11), 4792-4798. https://doi.org/10.1128/MCB.8.11.4792

Ludwig, L. S., Gazda, H. T., Eng, J. C., Eichhorn, S. W., Thiru, P., Ghazvinian, R., George, T. I., Gotlib, J. R., Beggs, A. H., Sieff, C. A., Lodish, H. F., Lander, E. S., & Sankaran, V. G. (2014). Altered translation of GATA1 in Diamond-Blackfan anemia. *Nature Medicine*, *20*(7), 748-753. https://doi.org/10.1038/nm.3557

Meskauskas, A., Russ, J. R., & Dinman, J. D. (2008). Structure/function analysis of yeast ribosomal protein L2. *Nucleic Acids Research*, *36*(6), 1826-1835. https://doi.org/10.1093/nar/gkn034

Mirabello, L., Khincha, P. P., Ellis, S. R., Giri, N., Brodie, S., Chandrasekharappa, S. C., Donovan, F. X., Zhou, W., Hicks, B. D., Boland, J. F., Yeager, M., Jones, K., Zhu, B., Wang, M., Alter, B. P., & Savage, S. A. (2017). Novel and known ribosomal causes of Diamond-Blackfan anaemia identified through comprehensive genomic characterisation. *Journal of Medical Genetics*, *54*(6), 417-425. https://doi.org/10.1136/jmedgenet-2016-104346

Mirabello, L., Macari, E. R., Jessop, L., Ellis, S. R., Myers, T., Giri, N., Alison, M., Mcgrath, K. E., Humphries, J. M., Ballew, B. J., Yeager, M., Joseph, F., He, J., Hicks, B. D., Burdett, L., Alter, B. P., Zon, L., & Sharon, A. (2014). Whole-exome sequencing and functional studies identifyRPS29 as a novel gene mutated in multi-case Diamond-Blackfan anemia families. *Blood*, *124*(May), 24-33. https://doi.org/10.1182/blood-2013-11-540278.The

Natchiar, S. K., Myasnikov, A. G., Kratzat, H., Hazemann, I., & Klaholz, B. P. (2017). Visualization of chemical modifications in the human 80S ribosome structure. *Nature*, *551*(7681), 472-477. https://doi.org/10.1038/nature24482

Parrella, S., Aspesi, A., Quarello, P., Garelli, E., Pavesi, E., Carando, A., Nardi, M., Ellis, S. R., Ramenghi, U., & Dianzani, I. (2014). Loss of GATA-1 full length as a cause of Diamond-Blackfan anemia phenotype. *Pediatric Blood & Cancer*, *61*(7), 1319-1321. https://doi.org/10.1002/pbc.24944

Pöll, G., Braun, T., Jakovljevic, J., Neueder, A., Jakob, S., Woolford, J. L., Tschochner, H., & Milkereit, P. (2009). rRNA maturation in yeast cells depleted of large ribosomal subunit proteins. *PloS One*, *4*(12), e8249. https://doi.org/10.1371/journal.pone.0008249

Reinsch, B., Grand, K., Lachman, R. S., Kim, H. K. W., & Sanchez-Lara, P. A. (2020). Expanding the phenotypic spectrum of RPL13-related skeletal dysplasia. *American Journal of Medical Genetics. Part A*. https://doi.org/10.1002/ajmg.a.61965

Ruggero, D., & Shimamura, A. (2014). Marrow failure: A window into ribosome biology. *Blood*, *124*(18), 2784-2792. https://doi.org/10.1182/blood-2014-04-526301

Sankaran, V. G., Ghazvinian, R., Do, R., Thiru, P., Vergilio, J.-A., Beggs, A. H., Sieff, C. A., Orkin, S. H., Nathan, D. G., Lander, E. S., & Gazda, H. T. (2012). Exome sequencing identifies GATA1 mutations resulting in Diamond-Blackfan anemia. *Journal of Clinical Investigation*, *122*(7), 2439-2443. https://doi.org/10.1172/JCI63597

Ulirsch, J. C., Verboon, J. M., Kazerounian, S., Guo, M. H., Yuan, D., Ludwig, L. S., Handsaker, R. E., Abdulhay, N. J., Fiorini, C., Genovese, G., Lim, E. T., Cheng, A.,

Cummings, B. B., Chao, K. R., Beggs, A. H., Genetti, C. A., Sieff, C. A., Newburger, P. E., Niewiadomska, E., … Gazda, H. T. (2018). The Genetic Landscape of Diamond-Blackfan Anemia. *The American Journal of Human Genetics*, *103*(6), 930-947. https://doi.org/10.1016/j.ajhg.2018.10.027

Vlachos, A., & Muir, E. (2010). How I treat Diamond-Blackfan anemia. *Blood*, *116*(19), 3715-3723. https://doi.org/10.1182/blood-2010-02-251090

Vlachos, A., Rosenberg, P. S., Atsidaftos, E., Alter, B. P., & Lipton, J. M. (2012). Incidence of neoplasia in Diamond Blackfan anemia: A report from the Diamond Blackfan Anemia Registry. *Blood*, *119*(16), 3815-3819. https://doi.org/10.1182/blood-2011-08-375972

Wang, R., Yoshida, K., Toki, T., Sawada, T., Uechi, T., Okuno, Y., Sato-Otsubo, A., Kudo, K., Kamimaki, I., Kanezaki, R., Shiraishi, Y., Chiba, K., Tanaka, H., Terui, K., Sato, T., Iribe, Y., Ohga, S., Kuramitsu, M., Hamaguchi, I., … Ito, E. (2015). Loss of function mutations in RPL27 and RPS27 identified by whole-exome sequencing in Diamond-Blackfan anaemia. *British Journal of Haematology*, *168*(6), 854-864. https://doi.org/10.1111/bjh.13229

Willig, T. N., Draptchinskaia, N., Dianzani, I., Ball, S., Niemeyer, C., Ramenghi, U., Orfali, K., Gustavsson, P., Garelli, E., Brusco, A., Tiemann, C., Pérignon, J. L., Bouchier, C., Cicchiello, L., Dahl, N., Mohandas, N., & Tchernia, G. (1999). Mutations in ribosomal protein S19 gene and diamond blackfan anemia: Wide variations in phenotypic expression. *Blood*, *94*(12), 4294-4306.

FIGURE LEGENDS

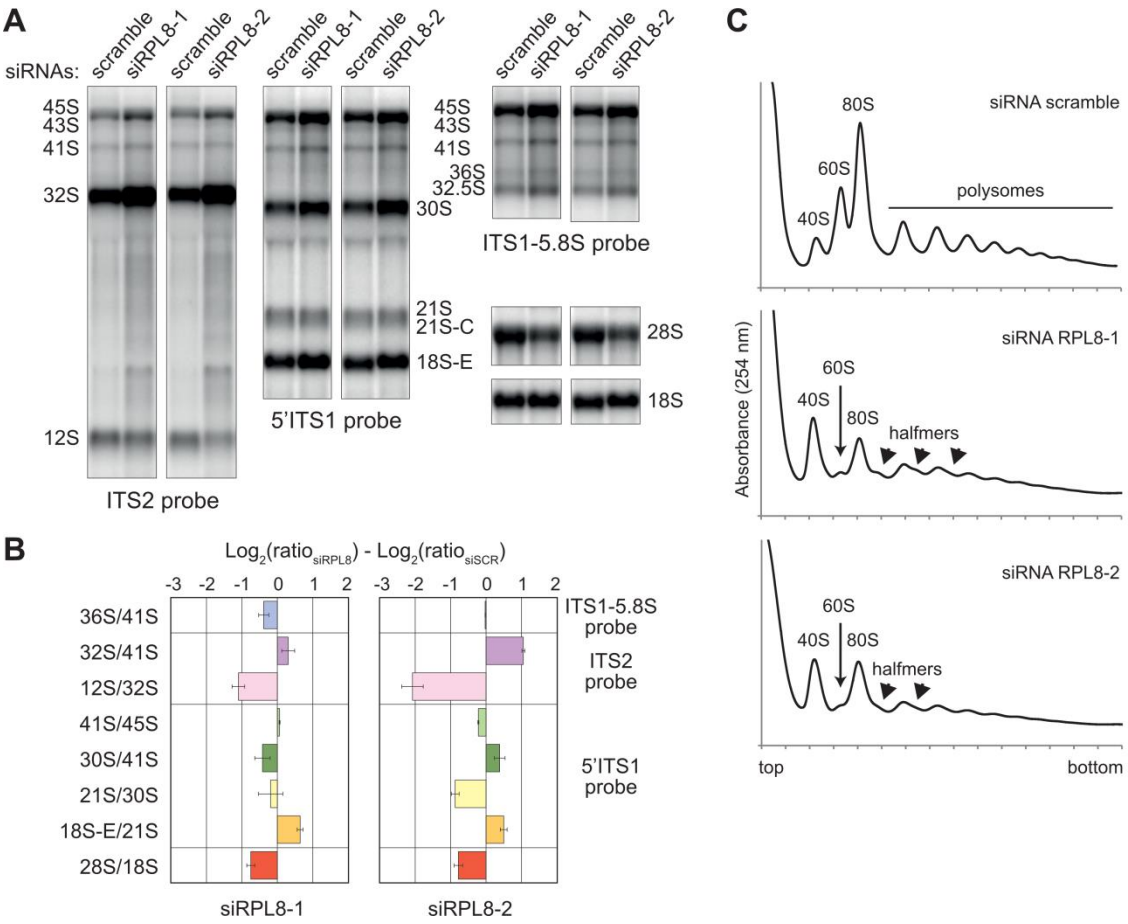

Figure 1. Knockdown of RPL8/uL2 impairs pre-rRNA processing and large ribosomal subunit production

HeLa cells were treated for 48 hours with two siRNA duplexes targeting *RPL8* mRNA expression. The *RPL8* mRNA was depleted by 89-95% with both siRNAs as assessed by RT-qPCR. (A) Total RNA extracts (3 µg/lane) were analyzed by northern blot after separation on a 1.1% agarose gel. After passive transfer, the membrane was sequentially hybridized with specific radiolabeled probes. (B) After quantification of the signals corresponding to the different rRNA precursors, $\log_2$ values of product to precursor ratios were expressed relative to control cells (n = 3). (C) After treating HeLa cells with cycloheximide for 10 min, cellular extracts were purified and analyzed on 10-50% sucrose gradients, in order to

separate small (40S) and large (60S) ribosomal subunits, monosomes (80S), and translating polysomes. The reduced free 60S subunit peaks in the profiles corresponding to siRPL8-treated cells are indicated with arrows, and halfmers are shown with arrowheads.

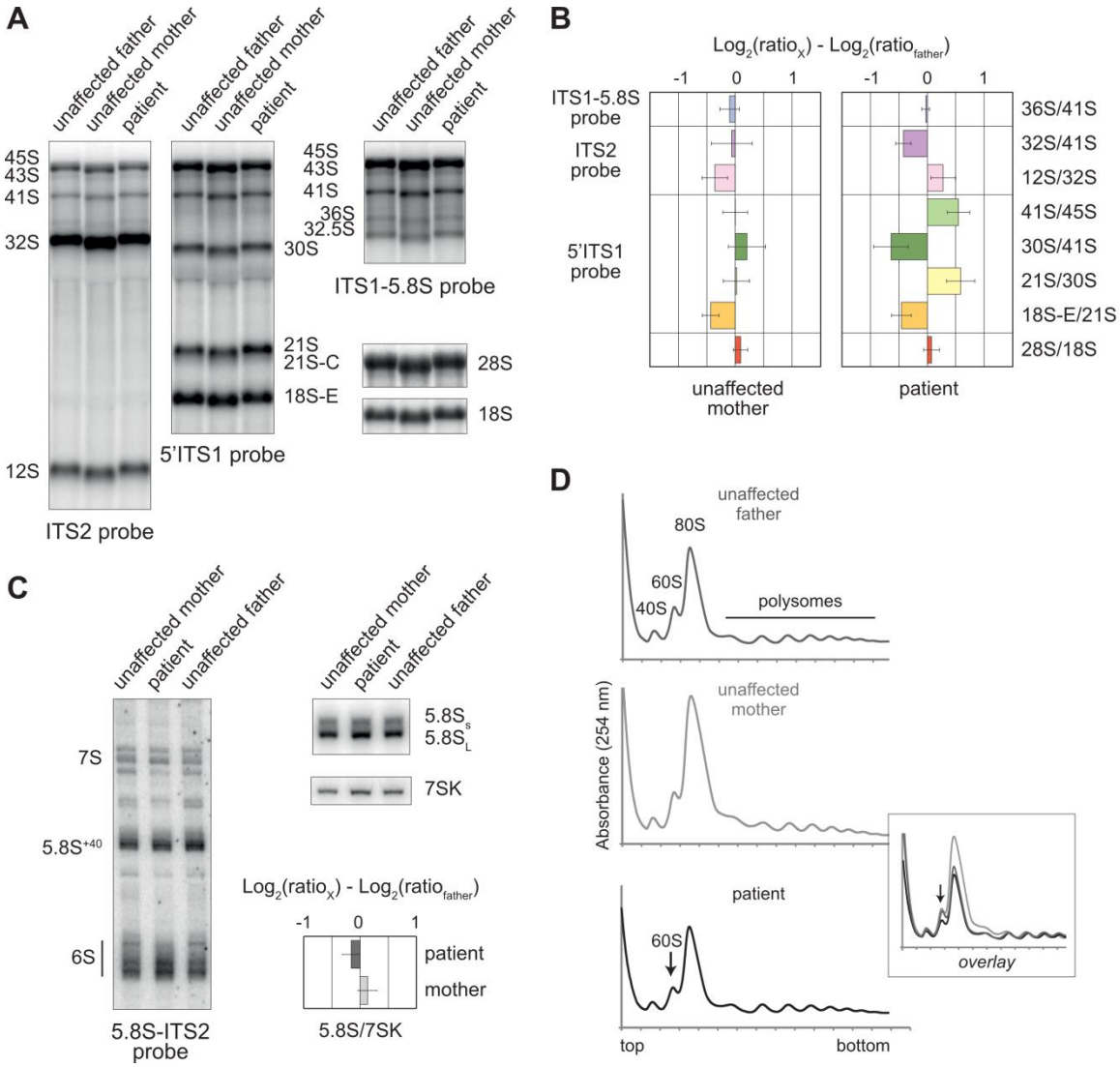

Figure 2. Analysis of ribosome biogenesis in cells expressing the RPL8/uL2 p.H38R variant

Pre-rRNAs were detected by northern blot in total RNA extracts prepared from LCLs derived from the unaffected father and mother and from the individual

expressing the p.H38R variant. (A) Pre-rRNAs (3 µg) were detected with various probes after separation on a 1.1% agarose gel. (B) Signals were quantified and are represented as $\log_2$ values of product to precursor ratios relative to the father's cells (n = 4 to 5). (C) Detection of precursors to the 5.8S rRNA after separation on a 6% denaturing polyacrylamide gel. The 5.8S signal was quantified as in (B) using the 7SK ncRNA as a reference. (D) After a 10 min treatment with cycloheximide, cellular extracts corresponding to a similar number of LCLs were analyzed on 10-50% sucrose gradients. The reduction of the free 60S subunit peak (corresponding to large ribosomal subunits) is pointed with an arrow in the patient profile. It is also superimposed with the profiles from the unaffected parents (inset). The experiment was repeated three times with similar results.

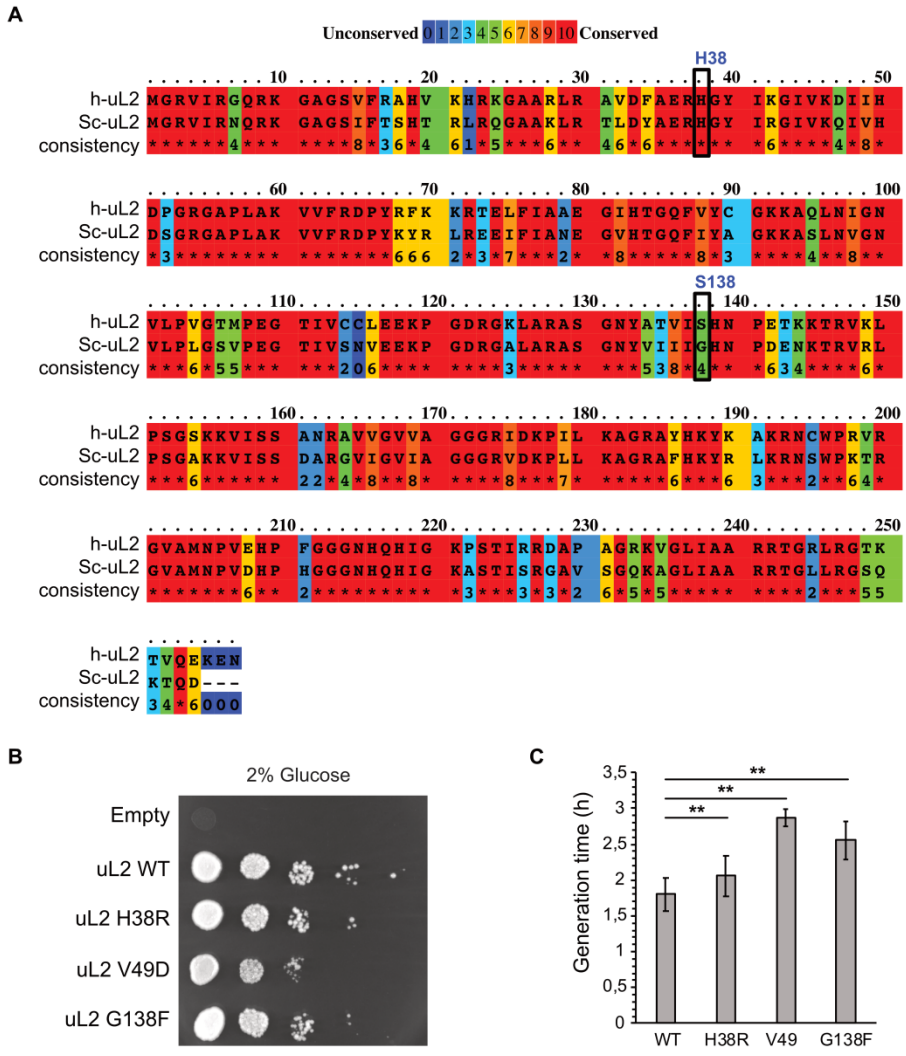

Figure 3. Different uL2 mutations result in variable growth defects

(A) Sequence alignment between *H. sapiens* and *S. cerevisiae* uL2 sequences by the PRALINE software. The color code indicates conservation level ranging from low (blue) to strong (red). (B) *GAL::RPL2* cells were transformed with centromeric plasmids directing expression of wild-type uL2 (uL2 WT), different uL2 mutants (p.H28R, p.G138F or p.V49D) or with the vector alone (Empty). Sequential ten-fold dilutions of the indicated cells were spotted either on YP agarose containing either galactose/sucrose or glucose, and incubated at 30°C for 3 days. (C) Generation times of the same strains as in B in liquid YP medium

containing glucose to repress expression of the chromosomic *RPL2* (means of four independent experiments). Paired t-tests were performed to compare the mutant strains with the wild-type strain (*: p-value < 0,05; ** p-value < 0,01; *** p-value < 0.001). The strain carrying the empty vector is not viable.

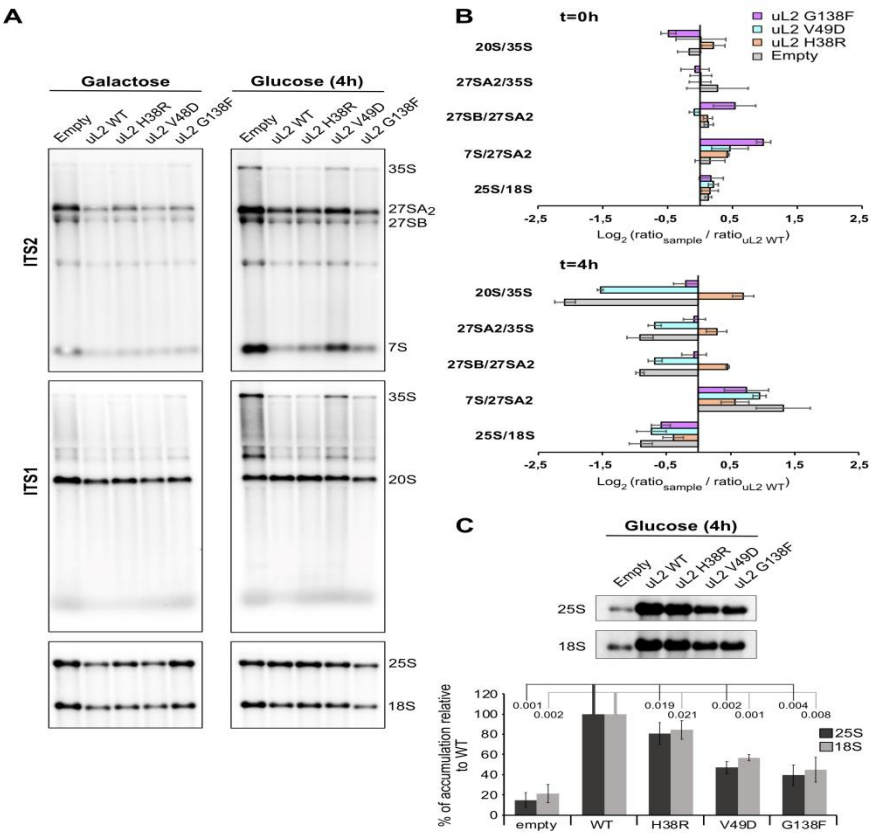

Figure 4. Alteration of pre-rRNA processing by the p.H38R and p.G138F uL2 mutants

(A) *GAL::RPL2* yeast cells expressing wild-type and mutated uL2 from a plasmid, or carrying an empty vector (Empty) were analyzed by northern blot after growth in galactose containing medium, or upon a 4 hour-shift to glucose containing medium to shut down chromosomal *RPL2*. Total RNAs (3 µg) were probed with radiolabeled oligonucleotides complementary to ITS2 (top panel), ITS1 (middle panel), or the 18S and 25S rRNAs (lower panel). The different intermediates in

pre-rRNA processing are described in Supp. Fig. S1. (B) Quantification of rRNA precursor ratios in three independent northern blot experiments. (C) Detection of 18S and 25S rRNAs in total RNAs extracted from the same amounts of cells for the different strains. The average accumulation of the 18S and 25S rRNAs, as determined from four independent experiments, is indicated as percentage of the levels observed in the wild-type strain. P-values on top the histogram correspond to paired t-tests performed to compare the mutant constructs with the wild-type.

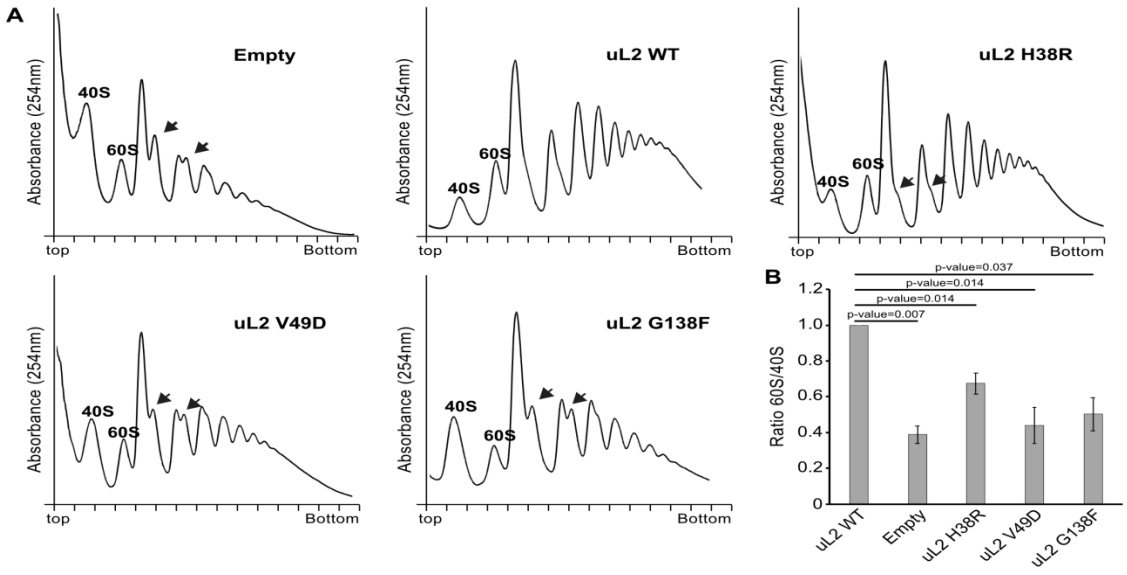

Figure 5. The p.H38R and p.G138F uL2 mutants affect 60S subunit accumulation

(A) Representative polysome profiles of *GAL::RPL2* yeast cells expressing the different variants of uL2 from a plasmid (Empty: vector alone). Halfmers are indicated by arrows. (B) Quantification of the ratios between the peaks corresponding to 60S and 40S free ribosomal subunits in polysome profiles from three independent experiments. The 60S/40S subunit ratio was arbitrarily set to 1

for the strain expressing wild-type uL2. P-values on top the histogram correspond to paired t-tests performed to compare the mutant constructs with the wild-type.

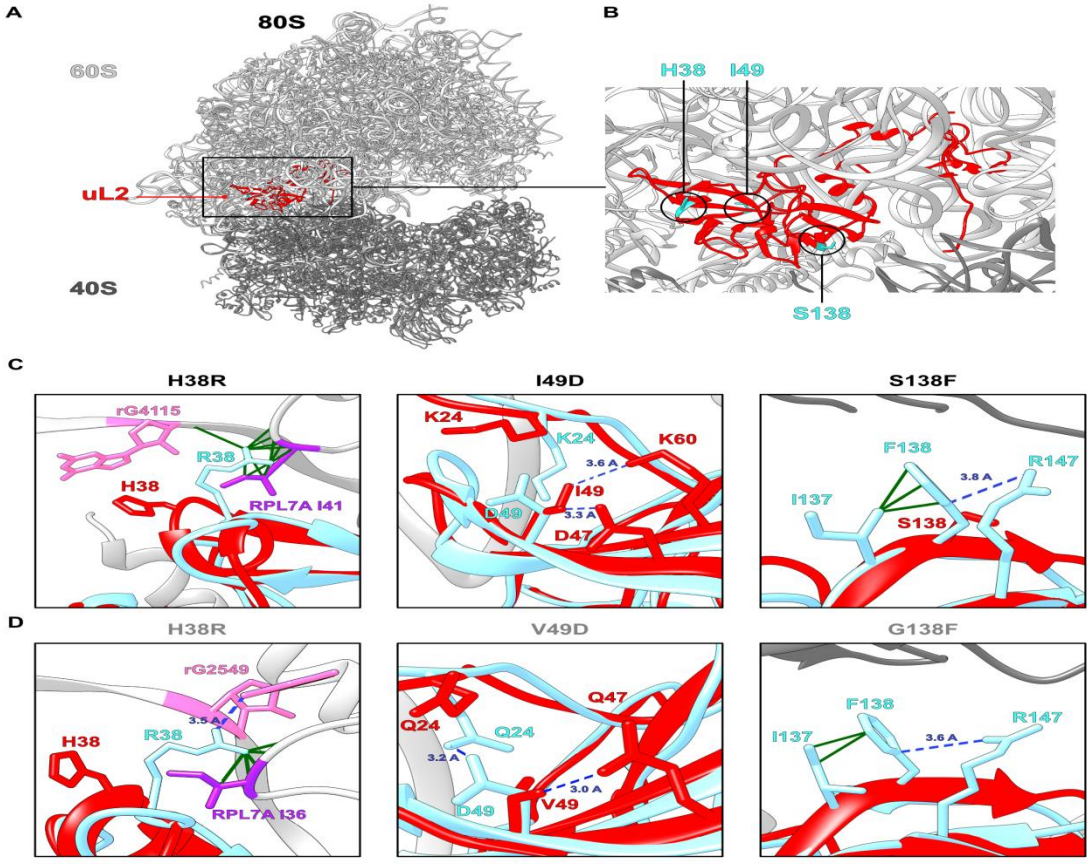

Figure 6. The p.H38R and p.S138F substitutions have different potential impacts on the structure of RPL8/uL2

(A) Structural organization of mature human 80S ribosomes solved by cryo-EM (pdb 6QZP; (Natchiar et al., 2017). RPL8/uL2 position in the large 60S subunit is shown in red. (B) Zoom on the ribosome structure centered around RPL8/uL2: the residues studied in this work are indicated in blue. (C) Molecular modeling of the RPL8/uL2 missense variants performed with the Phyre2 program (blue) is superimposed to the wild-type structure of RPL8/uL2 in the context of mature 80S ribosomes (red). Acquired bonds in the proximity of the mutations are

indicated (green), in addition distances between atoms located at close proximity that are gained or lost in mutants are indicated by blue dashed lines with distance in Angstrom on top. (D) As for human structures, the effects of point mutations on uL2 structure in the context of 80S ribosomes has been examined using yeast structure (6SNT) as a reference. The same color code is the same as as in (C).